Article:
Hirose, K., Nishio, K., TANAKA, S et al. (19 more authors) (2017) Role of Multichance Fission in the Description of Fission-Fragment Mass Distributions at High Energies. Physical Review Letters. 222501. ISSN 1079-7114

https://doi.org/10.1103/PhysRevLett.119.222501

A key role of multi-chance fission for the description of fission-fragment mass distributions at high energies

K. Hirose,[1,*] K. Nishio,[1] S. Tanaka,[2] R. Léguillon,[1] H. Makii,[1] I. Nishinaka,[1] R. Orlandi,[1] K. Tsukada,[1] J. Smallcombe,[3,1] M.J. Vermeulen,[1] S. Chiba,[4] Y. Aritomo,[2] T. Ohtsuki,[5] K. Nakano,[6] S. Araki,[6] Y. Watanabe,[6] R. Tatsuzawa,[7] N. Takaki,[7] N. Tamura,[8] S. Goto,[8] I. Tsekhanovich,[9] and A.N. Andreyev[10,1]

[1] *Advanced Science Research Center, Japan Atomic Energy Agency (JAEA), 2-4 Shirakata Shirane, Tokai, Ibaraki 319-1195 Japan*
[2] *Faculty of Science and Engineering, Kindai University, Higashi-Osaka 577-8502, Japan*
[3] *TRIUMF, Vancouver, British Columbia V6T 2A3, Canada*
[4] *Laboratory for Advanced Nuclear Energy, Institute for Innovative Research, Tokyo Institute of Technology, 2-12-1-N1-19, Ookayama, Meguro-ku, Tokyo 152-8550 Japan*
[5] *Research Reactor Institute, Kyoto University, Kumatori, Osaka 590-0494, Japan*
[6] *Interdisciplinary Graduate School of Engineering Sciences, Kyushu University, Fukuoka 816-8580, Japan*
[7] *Graduate School of Engineering, Tokyo City University, Tokyo 158-8557, Japan*
[8] *Graduate School of Science and Technology, Niigata University, Niigata 950-2181, Japan*
[9] *University of Bordeaux, 351 Cours de la Libration, 33405 Talence Cedex, France*
[10] *Department of Physics, University of York, York YO10 5DD, United Kingdom*

(Dated: October 12, 2017)

Fission-fragment mass distributions were measured for $^{237-240}$U, $^{239-242}$Np and $^{241-244}$Pu populated in the excitation-energy range from 10 to 60 MeV by multi-nucleon transfer channels in the reaction ^{18}O+^{238}U at the JAEA tandem facility. Among them, the data for ^{240}U and ^{240,241,242}Np were observed for the first time. It was found that the mass distributions for all the studied nuclides maintain a double-humped shape up to the highest measured energy in contrast to expectations of predominantly symmetric fission due to the washing out of nuclear shell effects. From a comparison with the dynamical calculation based on the fluctuation-dissipation model, this behavior of the mass distributions was unambiguously attributed to the effect of multi-chance fission.

PACS numbers: 25.70.Hi, 25.85.Ge, 27.90.+b

At present, about 11% of the world's electricity is produced by thermal-neutron-induced fission in nuclear power reactors. Management of nuclear waste, and in particular, of long-lived minor actinides produced in these reactors, is one of the most important issues in the use of nuclear power. For further public acceptance of nuclear power, it is essential to reduce the already-existing and newly-produced nuclear waste. The use of accelerator-driven systems (ADS), for example [1], is considered as one of the viable options for the incineration and/or transmutation of the long-lived minor actinides into shorter-lived fission products. In the ADS approach, energetic spallation neutrons, produced via high-energy proton impact on a heavy target material such as lead and/or bismuth, could be used to irradiate the fissionable minor actinides. This leads to fission with higher, and more broadly distributed, excitation energies in comparison to those in the thermal-neutron-induced fission in a traditional power reactor. Thus, understanding of fission at high excitation energy is important for nuclear-data evaluations related to ADS developments.

The fission process is usually described as an evolution of a nuclear shape on a potential-energy surface, resulting from the interplay of macroscopic nuclear properties and microscopic shell effects. The shape of fission-fragment mass distributions (FFMDs) is directly influenced by nuclear shell effects, a well-known example being the asymmetric FFMD in the thermal-neutron-induced fission of ^{235}U, whereby the compound nucleus, ^{236}U, fissions at the excitation energy of 6.55 MeV. The asymmetric FFMD, in this case, is attributed to the influence of strong shell effects in the fission fragments in the vicinity of doubly-magic ^{132}Sn.

With increasing excitation energy, two competing processes are expected to occur. First of all, due to a reduced importance of shell effects, the transition to predominantly symmetric (liquid-drop) type fission should occur, which is indeed demonstrated by many experiments [2]. The other process is multi-chance fission (MCF), or fission after consecutive neutron evaporations, where the fissioning nuclei with less neutrons will have lower excitation energy, thus showing stronger shell effects than in the initial compound nucleus. The latter effect is then supposed to favor the asymmetric fission of typical actinides after neutron evaporation. The MCF concept itself is well-known from studies of the fission probability in high-energy neutron-induced reactions, whereby step-like behavior is observed in the fission cross-sections at the energies corresponding to $1n$, $2n$, ... neutron emission (see for example Fig. 17 in [3]). It was also reported that the effects of MCF can be seen in the average total kinetic energy [4, 5], and in the average energy of the prompt fission neutrons [6], as a function of the excitation energy of the compound nuclei. In contrast to these

fission observables, to our knowledge, no experimental study of the effects of MCF on mass distributions has been reported to date. It was only recently that the effect of MCF on mass distributions was introduced in theoretical studies [7–10]. However, the validity of the calculated FFMDs for each fission chance was not shown because of the lack of experimental data. Thus, an elaborated and well justified interpretation of experimental FFMDs at high excitation energies has not been yet established.

In this Letter, we present our investigation of the effects of MCF on FFMDs, by measuring the mass distributions in a wide range of nuclides and excitation energies, using the novel experimental method recently developed at JAEA [11]. By exploiting multi-nucleon transfer (MNT) channels in the reaction ^{18}O+^{238}U, FFMDs of twelve isotopes of U, Np and Pu were obtained in the excitation energy range of E^*=10–60 MeV, some of which cannot be populated by other experimental methods. A persistence of predominantly asymmetric FFMDs was observed up to the highest measured excitation energy for all the studied nuclides. To understand this behavior, the fluctuation-dissipation model was used. It was shown that a reliable understanding of the observed FFMDs can be obtained only by invoking MCF.

The experiment was performed at the JAEA tandem accelerator facility using a 157.5 MeV ^{18}O beam with an intensity of 0.5 pnA. The target was prepared by electrodeposition of an 80 μg/cm^2 layer of ^{238}U on a 90 μg/cm^2 nickel backing. The experimental setup, consisting of a multi-detector ΔE-E silicon telescope and four multi-wire proportional counters (MWPCs) for ejectile and fission-fragment measurements, respectively, is described in [11], thus only a brief description is given here.

Specific particle-transfer channels were determined by identifying the ejectiles using the array of ΔE-E silicon detectors. An ejectile passing through one of the twelve ΔE detectors (75 μm thick) is stopped in the E detector (300 μm thick) to measure the residual energy ($E_{\rm res}$, $E_{\rm tot}$=ΔE+$E_{\rm res}$). The angle of the ejectile was determined by the combination of a ΔE segment and one of the 16 annular strips in the E detector where the ejectile was detected. The unique feature of the JAEA setup is the good energy resolution of the ΔE detectors which was achieved by using silicon wafers of highly uniform thickness (<1.3% variation). This feature allowed us to distinguish not only the ejectiles of different elements (*e.g.* O, N, C...), but also different isotopes of each element, as shown in Fig. 1. This figure shows the detected ejectiles plotted on the $E_{\rm tot}$-ΔE plane, where a clear separation of neighboring isotopes of the same element is seen. A possible contamination from neighboring isotopes was estimated for each excitation-energy range with a 10-MeV interval from 10 to 60 MeV, and found to be on the level

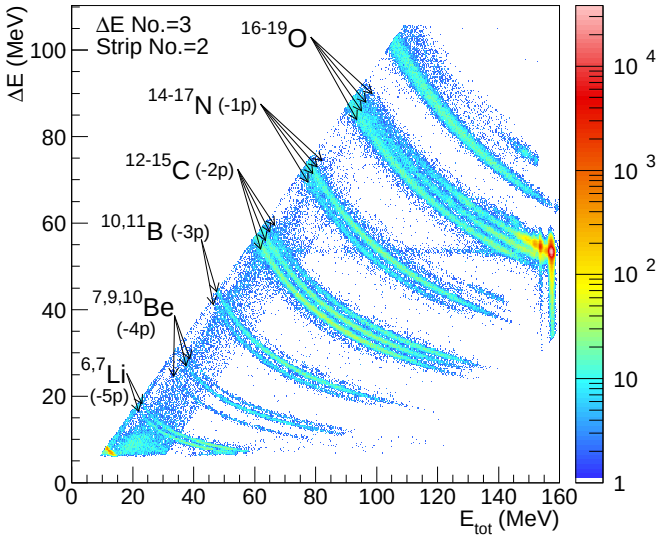

FIG. 1. (Color online) ΔE-$E_{\rm tot}$ spectrum for ejectiles measured in the reaction ^{18}O+^{238}U for one combination of the ΔE-E detectors (ΔE segment No. 3 and E annular strip No. 2). The curves corresponding to different ejectiles are labeled with the respective isotopes.

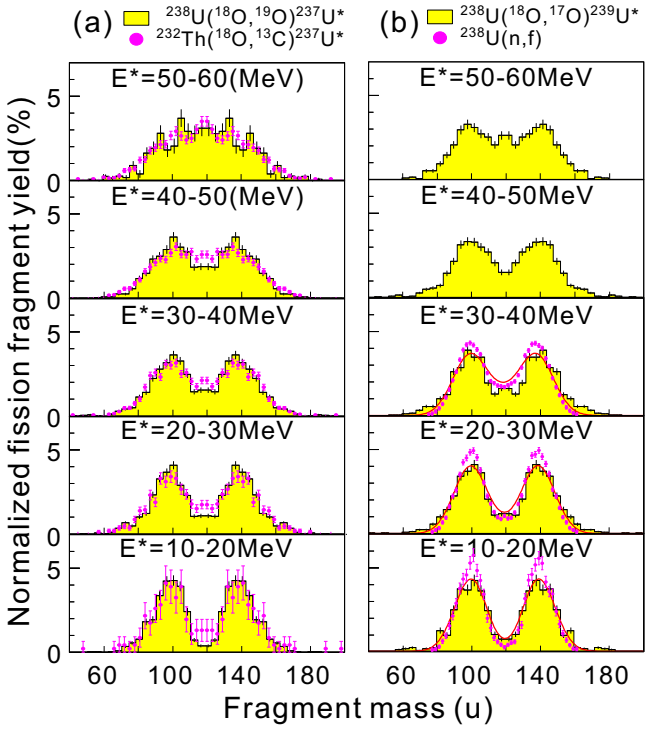

FIG. 2. (Color online) (a) FFMDs for ^{237}U populated by ($-1n$) channel in the present study (yellow histograms) and by ($+2p3n$) channel in the reaction ^{18}O+^{232}Th (closed circles [11]). (b) The same for ^{239}U from the present study (yellow histogram) in comparison to those from n+^{238}U [12] (closed circles). The red curves are the FFMDs from [12] which are broadened according to the mass resolution, see text.

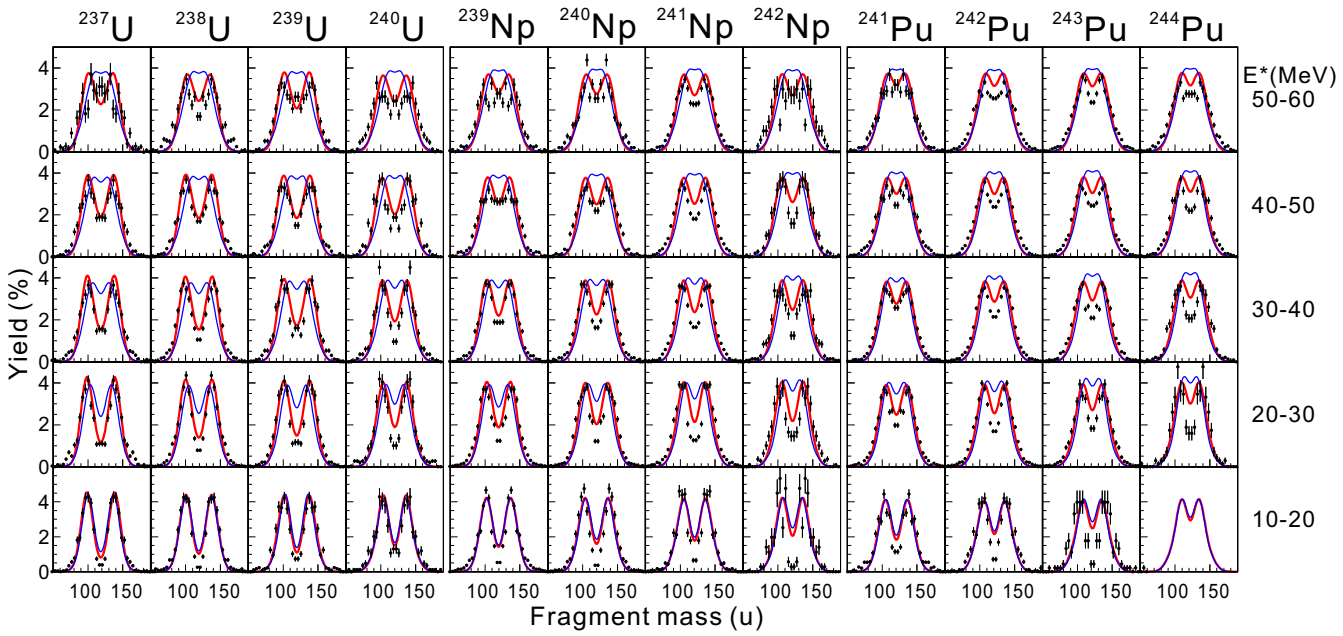

FIG. 3. (Color online) Experimental FFMDs (points with error bars) of the U, Np and Pu isotopes and their dependence on excitation energy in the range of E^*=10–60 MeV. The FFMD for ^{244}Pu at the lowest excitation-energy bin is not shown due to statistical reasons. The experimental FFMDs are compared with Langevin calculations respectively without (blue curves) and with (red curves) the inclusion of multi-chance fission (see text).

of 6%, 3% and 2% on average, for $^{16-19}$O, $^{14-17}$N and $^{12-15}$C, respectively. There were two cases with a less evident separation, *i.e.*, ^{19}O (^{237}U) and ^{18}O (^{238}U) at E^*=50–60 MeV, where the admixture of neighboring isotopes was as high as ∼25%. To obtain the correct FFMD of ^{238}U, the FFMD of the major contaminant ^{239}U (23%) was subtracted from the initially derived FFMD for ^{238}U. The data for ^{237}U was obtained in the same manner, by subtracting the contribution of ^{238}U (25%) which is the only background source. In the analysis, it was found that the change in the FFMDs by the background correction remained within the statistical errors and did not alter the shapes of the FFMDs. Hence, the background subtraction was not applied to the rest of the data.

The momentum of the recoiling compound-nucleus, which should be shared by both fragments in fission, was determined from the energy $E_{\rm tot}$ and the direction of the ejectile. The excitation energy of the compound nucleus was then deduced from the recoil momentum, $E_{\rm tot}$, and the reaction Q-value [13]. It is assumed that no excitation energy is given to the ejectile, thus the excitation energies quoted in this study should be considered as the upper limit. The measured resolution for $E_{\rm tot}$ is ∼1.0 MeV (FWHM), which determines the uncertainty of the excitation energy of a compound nucleus. Coincident fission fragments produced in MNT fission were detected by using position-sensitive MWPCs, which allow determination of the directions of the fission fragments. The time of flight difference between two fragments was measured to determine the pre-neutron-emission masses.

As an example of benchmarking of the method and new data, in Fig. 2 FFMDs for (a) ^{237}U ($-1n$ transfer) and (b) ^{239}U ($+1n$ transfer) from our experiment are compared with the existing data [11, 12]. The closed circles in Fig. 2(a) show FFMDs for ^{237}U observed in our previous measurement of the $+2p3n$-transfer channel in the reaction ^{18}O+^{232}Th [11] using the same experimental setup. A fairly good agreement, both for mass asymmetry and for peak-to-valley (P/V) ratio, at all measured excitation energies may imply the independency of the FFMDs from the transfer channel. In Fig. 2(b), FFMDs for ^{239}U are compared to those deduced in the neutron-induced fission of ^{238}U [12] (closed circles) at the similar excitation energy ranges of E^*=13.8–15.8 MeV, 18.8–23.8 MeV and 30.8–44.8 MeV. They have a mass resolution of 3.5 u in average, estimated from their spectra [14]. To allow for comparison with the present data (mass resolution σ=6.5 u), their FFMDs were broadened and the results are shown by the red curves in Fig. 2(b). For the two lowest energy regions, the P/V ratios obtained from their broadened FFMDs showed a good agreement with those from the present data within the statistical errors. Their P/V ratio at E^*=20–30 MeV was found to be about 20% larger than our value of 2.3 ± 0.2, but still agrees within two sigma. As shown in Fig. 2, the MNT reaction provides the opportunity to study poorly-understood spin dependence in fission. Although detailed studies are needed to find the conditions for which the present MNT approach could be used as a surrogate for neutron-induced fission, the reached agreements with the

other experimental methods indicate that a set of FFMDs shown later have enough quality to discuss the effect of MCF.

As a summary of all the experimental results, Fig. 3 shows the FFMDs for the twelve compound nuclides $^{237-240}$U, $^{239-242}$Np and $^{241-244}$Pu obtained by gating on the different ejectiles (*i.e.*, different MNT channels) in Fig. 1. A 10-MeV interval of the excitation energy was chosen as a compromise between the available statistics and a reasonable increment of E^*. It should be noted that the FFMDs for ^{240}U and ^{240,241,242}Np were observed for the first time. It is evident that the FFMDs for all nuclides in Fig. 3 have predominantly asymmetric shape at the lowest excitation energy. A growing contribution of symmetric fission can be observed with increasing excitation energy, however the double-humped shapes are still clearly preserved.

To understand these trends, the experimental FFMDs are compared with a calculation based on the fluctuation-dissipation fission model developed in [15, 16]. In this model, the evolution of a nuclear shape, defined by three parameters (charge-center distance, mass-asymmetry and fragment deformation), is traced from the compound state to the scission point by solving the Langevin equations, and FFMDs are calculated with the Monte Carlo method. The potential energy is defined as the sum of the liquid-drop part and excitation-energy (E^*)-dependent shell-correction energy given by: $\delta W(0)\times\exp(-E^*/E_d)$, where $\delta W(0)$ is the zero-excitation shell-correction energy. The shell-damping energy was chosen to be E_d=20 MeV, as in [11, 16]. The calculation reproduces well the global shape the FFMDs, both for the peak-to-valley ratio of the double-humped shape and the position of the light and heavy-fragment peaks, for n+^{233,235}U, ^{239}Pu [16] as well as our recent MNT fission data for $^{231-234}$Th, $^{232-236}$Pa and $^{234-238}$U [11] within the limit of low excitation energies E^* $\leq$20 MeV, for which the effects of MCF should be small.

As a first step in the present calculations, MCF was not taken into account, which means that calculated FFMDs are due only to fission of the initial compound nucleus at each specific excitation energy. The results are shown by the thin blue curves in Fig. 3. Under this assumption, the mass asymmetry, *i.e.*, the peak positions of the double-humped FFMD, for all isotopes are reproduced below $E^*\sim$20 MeV, with clear deviations seen for higher energies. At the highest energy, the calculation shows structure-less symmetric fission in contrast to the measurement. With regard to the P/V ratios of the FFMDs at E^*=10–20 MeV, the calculation which reproduced those for $^{231-234}$Th, $^{232-236}$Pa and $^{234-237}$U from the MNT fission of ^{18}O+^{232}Th [11] agrees well also with the present data for the heavier uranium isotopes $^{238-240}$U. On the contrary, the calculation gives a smaller P/V ratio for heavier neptunium (^{241,242}Np) and plutonium ($^{241-244}$Pu) isotopes. One of the possible reasons for this deviation could be in the treatment of the neck parameter ε ($0 < \varepsilon < 1$) [17], which defines the depth of the potential at the neck of the dumbbell-shaped nucleus, used in our two-center shell calculation. In this work, we adopted ε=0.35 derived as an optimal value in [16] to explain the FFMDs of compound nuclei with mass of 234–240. For heavier nuclei, this value could thus be slightly different. This deviation, however, does not influence our conclusion which was drawn from the discussion on the excitation-energy dependence of the FFMDs. The evolution of the ε parameter in heavier nuclei will be the topic of a future investigation.

In the next step, MCF was introduced into the calculation. Figure 4(a) is a conceptual view of MCF for the case of ^{240}U as the initial compound nucleus. The highly excited ^{240}U can decay either via first-chance fission, or via single neutron emission, leading to the less excited ^{239}U. The latter nucleus can decay again either by fission (thus, second-chance fission) or by neutron evaporation; the competition between fission and neutron emission continues until the excitation energy drops below the fission barrier of the corresponding daughter nucleus. The shape of the FFMD at each fission chance is also shown schematically in this panel, with predominantly symmetric fission for the initial highly excited compound nucleus ^{240}U, and dominant asymmetric fission for subsequent fission chances of daughter nuclides, in particular, for ^{237}U (4th-chance fission). The application of this procedure to the calculated FFMDs for ^{240}U* is demonstrated in Fig. 4(b). The calculated FFMDs for respective fission chances are shown by the dashed curves with different colors, where the fraction (probability) of each fission chance is determined using the GEF code [8]. The reduction of the excitation energy of the compound nucleus due to neutron emission was calculated from neutron binding energies [18] and a mean energy for the emitted neutron, $\sim$1.9 MeV, obtained by the PACE2 code [19]. For each MCF step, the potential energy surface of the respective compound nucleus was also adopted. The sum of all the FFMDs obtained from each fission chance (up to 6th-chance fission) is shown by the thin black curve. It reproduces the observed peak positions of the experimental FFMD, but has narrower peaks than the measured ones. However, after introducing the experimental mass resolution, the calculation well reproduces also the P/V ratio as well as the mass asymmetry as shown by the thick solid red curve. The key conclusion which can be drawn from Fig. 4(b) is that the *apparent* mass-asymmetric fission observed in the data even at high excitation energies originates from the lower-energy 4th-, 5th-, and 6th-chance fissions (^{235,236,237}U). On the contrary, the 1st- and 2nd-chance fissions lead to predominantly symmetric mass splits, as they occur at high excitation energy.

The same calculation procedure was applied to all the cases displayed in Fig. 3, where the results are shown by thick red curves. In contrast to the results without MCF

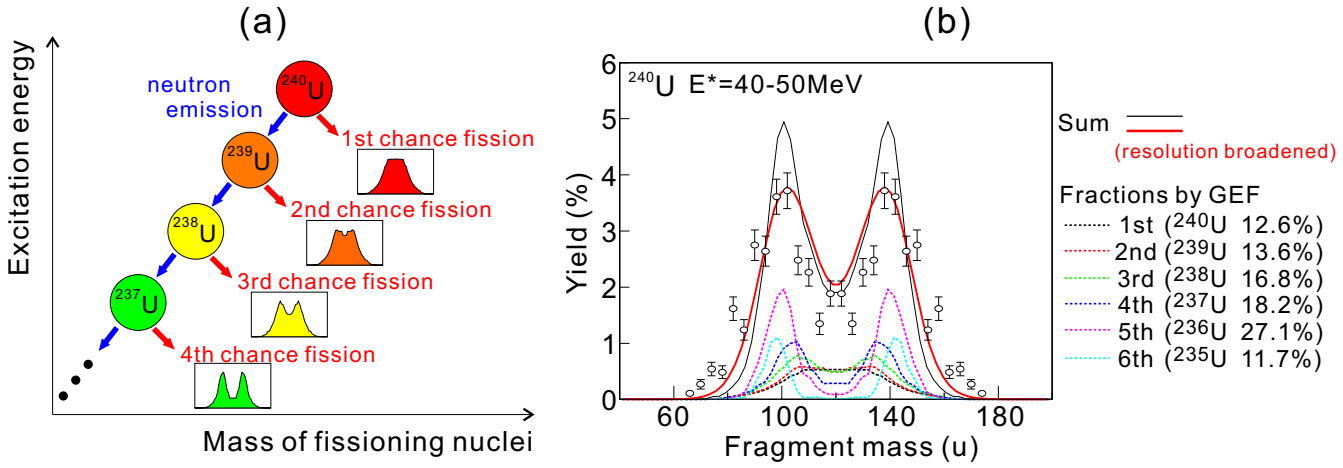

FIG. 4. (Color online) (a) A conceptual view of MCF for the case of ^{240}U*, see details in the text. (b) Calculated FFMDs for all the MCF steps up to 6th-chance fission (dashed curves) are shown for the initial compound nucleus ^{240}U at excitation energies of 40–50 MeV. Their sum is given by the thin solid line. For comparison with the experimental data (open symbols with error bars), the calculated sum of the FFMDs was broadened by the experimental mass resolution, and the resulting FFMD is shown by the red thick curve.

(thin blue curves), the calculation with MCF well explains the excitation-energy dependence of the FFMDs characterized by mass-asymmetry and P/V ratio. With increasing excitation energy, FFMDs contain greater contributions from higher fission chances. Therefore, the agreement in Fig. 3 for all the excitation-energy ranges validates the calculation of the FFMDs. The decreasing P/V ratio of the measured FFMDs from uranium to plutonium (for example, E^*=30–40 MeV) is also explained by introducing MCF, whereas the analysis without MCF predicts almost the same flat-top distributions through all the isotopes.

To conclude, even though MCF is a well-established concept in several fission observables (*e.g.* fission probability), so far its role for fission-fragment mass distributions has not been experimentally investigated. This is mainly due to the absence of systematic data on the FFMDs in a large span of excitation energies. We overcame this difficulty by exploiting the novel approach of multi-nucleon transfer reactions. Fission of a multitude of nuclides studied in a broad range of excitation energies has allowed us to show that the *apparent* asymmetric shape of FFMDs for a given initial excitation energy originates from fission of less excited lighter isotopes produced via a chain of MCF. In particular, this finding means that asymmetric shapes in the FFMDs measured at high excitation energies ($E^*>S_n$) should no longer be interpreted as signatures of survival of shell effects in the initial compound nucleus, which would incite one to reexamine existing experimental data measured at high excitation energies. Ignoring multi-chance fission, the asymmetric structure of FFMD observed at high excitation energy would introduce an unexpectedly higher shell-damping energy than the conventional E_d=20 MeV which was also used in this work. The shell-correction energy at high excitation energy is also important for other fields, for example, heavy-ion fusion reaction for the synthesis of super-heavy elements (SHEs). This is because only the shell-correction energy forms the fission barrier of a compound nucleus the height of which significantly alters its survival probability in the competition between neutron evaporation and fission.

Our results also suggest that the consideration of MCF is essential to interpret and evaluate other fission observables. One of the examples is the neutron multiplicity as a function of fragment mass A, $\bar{\nu}(A)$. An important, but not yet fully understood phenomenon, the increase of the initial excitation energy leads to enhancement of $\bar{\nu}(A)$ only for heavy fragments [8, 20]. For a quantitative discussion, $\bar{\nu}(A)$ should be also represented as a sum of contributions from each fission chance. As a further development of our MNT approach, we aim to undertake measurements of prompt neutrons correlated with fission fragments by installing a neutron-detector array around the present fission setup.

The authors would like to thank the crew of the JAEA-tandem accelerator facility for their beam operation. Present study is supported by "Comprehensive study of delayed-neutron yields for accurate evaluation of kinetics of high burn-up reactors" and "Development of prompt-neutron measurement in fission by surrogate reaction method and evaluation of neutron-energy spectra" by the Ministry of Education, Culture, Sports, Science and Technology of Japan (MEXT). This work was partly done within an IAEA CRP on beta-delayed neutrons (F41030). The Langevin calculations have been done using the cluster computer system (Kindai-VOSTOK) which is supported by "Research funds for External Fund

Introduction (2015-16)" by Kindai University. This work was also supported partly by STFC of UK.

* hirose.kentaro@jaea.go.jp

[1] T. Mukaiyama, T. Takizuka, M. Mizumoto, Y. Ikeda, T. Ogawa, A. Hasegawa, H. Takada, and H. Takano, Prog. Nucl. Energy **38**, 107 (2001).

[2] C. Wagemans, ed., The Nuclear Fission Process (CRC Press, 1991).

[3] K. Shibata, O. Iwamoto, T. Nakagawa, N. Iwamoto, A. Ichihara, S. Kunieda, S. Chiba, K. Furutaka, N. Otuka, T. Ohsawa, T. Muraya, H. Matsunobu, A. Zukeran, S. Kamada, and J. Katakura, Journal of Nuclear Science and Technology **48**, 1 (2011).

[4] J. Lestone and T. Strother, Nuclear Data Sheets **118**, 208 (2014).

[5] D. L. Duke, F. Tovesson, A. B. Laptev, S. Mosby, F.-J. Hambsch, T. Bryś, and M. Vidali, Phys. Rev. C **94**, 054604 (2016).

[6] T. Ethvignot, M. Devlin, H. Duarte, T. Granier, R. C. Haight, B. Morillon, R. O. Nelson, J. M. O'Donnell, and D. Rochman, Phys. Rev. Lett. **94**, 052701 (2005).

[7] M. C. Duijvestijn, A. J. Koning, and F.-J. Hambsch, Phys. Rev. C **64**, 014607 (2001).

[8] K.-H. Schmidt, B. Jurado, C. Amouroux, and C. Schmitt, Nuclear Data Sheets **131**, 107 (2016), special Issue on Nuclear Reaction Data.

[9] M. D. Usang, F. A. Ivanyuk, C. Ishizuka, and S. Chiba, Phys. Rev. C **94**, 044602 (2016).

[10] P. Möller and C. Schmitt, The European Physical Journal A **53**, 7 (2017).

[11] R. Léguillon, K. Nishio, K. Hirose, H. Makii, I. Nishinaka, R. Orlandi, K. Tsukada, J. Smallcombe, S. Chiba, Y. Aritomo, T. Ohtsuki, R. Tatsuzawa, N. Takaki, N. Tamura, S. Goto, I. Tsekhanovich, C. M. Petrache, and A. N. Andreyev, Physics Letters B **761**, 125 (2016).

[12] V. D. Simutkin, S. Pomp, J. Blomgren, M. Österlund, R. Bevilacqua, P. Andersson, I. V. Ryzhov, G. A. Tutin, S. G. Yavshits, L. A. Vaishnene, M. S. Onegin, J. P. Meulders, and R. Prieels, Nuclear Data Sheets **119**, 331 (2014).

[13] G. Audi, M. Wang, A. Wapstra, F. Kondev, M. MacCormick, X. Xu, and B. Pfeiffer, Chinese Phys. C **36**, 1287 (2012).

[14] V. D. Simutkin, Ph.D. thesis, Uppsala University (2010).

[15] V. Zagrebaev and W. Greiner, Journal of Physics G: Nuclear and Particle Physics **31**, 825 (2005).

[16] Y. Aritomo and S. Chiba, Phys. Rev. C **88**, 044614 (2013).

[17] K. Sato, A. Iwamoto, K. Harada, S. Yamaji, and S. Yoshida, Zeitschrift für Physik A Atoms and Nuclei **288**, 383 (1978).

[18] P. Möller, A. Sierk, T. Ichikawa, and H. Sagawa, Atomic Data and Nuclear Data Tables **109 - 110**, 1 (2016).

[19] A. Gavron, Phys. Rev. C **21**, 230 (1980).

[20] G. N. Kniajeva, L. Krupa, A. A. Bogachev, G. G. Chubarian, O. Dorvaux, I. M. Itkis, M. G. Itkis, J. Kliman, S. Khlebnikov, N. A. Kondratiev, E. M. Kozulin, V. Lyapin, T. Materna, I. V. Pokrovsky, V. A. Rubchenya, W. H. Trzaska, D. Vakhtin, and V. M. Voskressenski, Nuclear Physics A **734, Supplement**, E25 (2004), proceedings of the Eighth International Conference on Nucleus-Nucleus Collisions (NN2003).